

Semiquantitative Assessment of Intratumoral Susceptibility Signals Using Non-Contrast-Enhanced High-Field High-Resolution Susceptibility-Weighted Imaging in Patients with Gliomas: Comparison with MR Perfusion Imaging

ORIGINAL RESEARCH

M.J. Park
H.S. Kim
G.-H. Jahng
C.-W. Ryu
S.M. Park
S.Y. Kim

BACKGROUND AND PURPOSE: It has been reported that high-resolution susceptibility-weighted imaging (HR-SWI) may demonstrate brain tumor vascularity. We determined whether the degree of intratumoral susceptibility signal intensity (ITSS) on HR-SWI correlates with maximum relative cerebral blood volume (rCBVmax) and to compare its diagnostic accuracy for glioma grading with that of dynamic susceptibility contrast (DSC) perfusion MR imaging.

MATERIALS AND METHODS: Forty-one patients with diffuse astrocytomas underwent both non-contrast-enhanced HR-SWI and DSC at 3T. We correlated the degree and morphology of ITSS with rCBVmax within the same tumor segment. The degree of ITSS and rCBVmax were compared among 3 groups with different histopathologic grades. Spearman correlation coefficients were determined between the degree of ITSS, rCBVmax, and glioma grade. Receiver operating characteristic (ROC) curve analyses were performed to determine the diagnostic accuracy for glioma grading.

RESULTS: The degree of ITSS showed a significant correlation with the value of rCBVmax in the same tumor segments ($r = 0.72$, $P < .0001$). However, the areas of densely prominent ITSSs did not accurately correspond with those of rCBVmax. Spearman correlation coefficients between ITSS degree and glioma grade were 0.88 (95% confidence interval, 0.79–0.94). In the ROC curve analysis of histopathologic correlation by using the degree of ITSS, the optimal sensitivity, specificity, positive predictive value, and negative predictive value for determining a high-grade tumor were 85.2%, 92.9%, 95.8%, and 76.5%, respectively.

CONCLUSIONS: The degree of ITSS shows a significant correlation with the value of rCBVmax in the same tumor segments, and its diagnostic performance for glioma grading is comparable with that of DSC.

High-resolution susceptibility-weighted imaging (HR-SWI) has been recently reported to demonstrate magnetic susceptibility differences of various tissues that use blood oxygen level-dependent (BOLD) signal-intensity-induced phase differences between venous blood and surrounding brain parenchyma.¹⁻³ HR-SWI can increase the sensitivity to susceptibility effects of microvenous structures and blood products. Therefore, this novel imaging technique can be used in non-invasive visualization of normal or pathologic vascular structures that are not visible in conventional MR imaging.⁴

So far, HR-SWI has mainly been used in the assessment of various vascular and hemorrhagic brain disorders, such as arteriovenous malformations, occult low-flow vascular lesions, and cavernous malformations.⁴⁻⁶ The clinical application of this novel technique with a 1.5T MR imaging scanner, however, has been limited by long acquisition times related to relatively long TEs, which are required for the BOLD-induced phase effect. This long acquisition time can lead to motion artifacts, and the use of HR-SWI at 1.5T can be time-consuming in a routine MR imaging protocol. Recently, the develop-

ment of a 3T MR imaging scanner and parallel imaging techniques made it possible to increase the speed, coverage, and signal intensity-to-noise ratio of MR imaging. Therefore, this novel technique is now suitable for the examination of patients with various brain disorders to obtain both a high spatial resolution and a reasonable acquisition time. Moreover, HR-SWI can provide much additional information compared with a conventional gradient-echo imaging.

In gliomas, angiogenesis has been shown to be associated with tumoral viability and aggressiveness. Currently dynamic susceptibility-weighted contrast-enhanced perfusion MR imaging (DSC) provides information about neovascularity and angiogenesis in gliomas.⁷⁻⁹ Relative cerebral blood volume (rCBV) and vascular permeability measurements (K^{trans}) correlate significantly with glioma grading, as determined by histopathology.⁷⁻⁹ On the other hand, Mittal et al¹⁰ proposed that high rCBV values on perfusion imaging in tumors go hand in hand with evidence of blood products detected within the tumor matrix on HR-SWI. However, larger comparative studies of perfusion imaging and HR-SWI are needed to determine a more precise role of HR-SWI in the grading of cerebral neoplasms. Pinker et al¹¹ reported that the intratumoral susceptibility signal intensity (ITSS) on HR-SWI correlated with tumor grade as determined by positron-emission tomography (PET) studies and histopathology; therefore, this imaging technique seems to be a promising tool for noninvasive glioma grading.¹²

Our hypothesis is that the detection of ITSS in higher grade

Received October 30, 2008; accepted after revision February 11, 2009.

From the Department of Diagnostic Radiology (M.J.P., H.S.K., S.M.P., S.Y.K.), Ajou University School of Medicine, Suwon, Korea; and Department of Radiology (G.-H.J., C.-W.R.), East-West Neo Medical Center, Kyunghee University School of Medicine, Seoul, Korea.

Please address correspondence to Ho Sung Kim, MD, Department of Diagnostic Radiology, Ajou University School of Medicine, Mt 5, Woncheon-dong, Yeongtong-gu, Suwon, Gyeonggi-do, 442-749; Korea, e-mail: J978005@lycos.co.kr

DOI 10.3174/ajnr.A1593

gliomas not only reflects tumor vascularity but also indicates considerable susceptibility in areas of macro- and micro-necrosis in higher grade gliomas. In the present study, we assessed whether the ITSS on HR-SWI correlates with qualitative and quantitative rCBV values on DSC and compared the diagnostic accuracy for glioma grading between HR-SWI and DSC.

Materials and Methods

Study Patients

Forty-one consecutive patients with histologically proved diffuse astrocytomas were enrolled in this study. All study patients underwent HR-SWI, DSC, and conventional MR imaging before surgical biopsy and/or resection. There were 19 male and 22 female patients, with ages ranging from 19 to 70 years and a mean age of 47 years. An experienced neuropathologist performed the histopathologic evaluations. Pathologic specimens had been obtained by means of either stereotactic resection ($n = 29$) or stereotactically guided biopsy ($n = 12$) and were classified in accordance with the revised WHO system of brain tumors.¹³ In our study, we excluded oligodendrogliomas, which could confound the correlation between the degree of ITSS and the maximum rCBV value (rCBVmax). The local institutional review board approved our study, and informed consent was obtained from all patients or members of their families.

MR Imaging Protocol

MR imaging was performed by using a 3T MR imaging scanner (Achieva; Philips Medical Systems, Best, the Netherlands) with a dedicated 8-channel sensitivity encoding head coil. Standard MR imaging included the following sequences: axial fast spin-echo T2-weighted imaging (TR/TE, 3000/80 ms), axial spin-echo T1-weighted imaging (TR/TE, 495/10 ms), and contrast-enhanced axial and coronal T1-weighted imaging. The contrast-enhanced axial and coronal T1-weighted sequences were performed after administering 0.1 mmol/kg of gadopentetate dimeglumine (Magnevist; Schering, Berlin, Germany) per kilogram of body weight.

HR-SWI was performed according to the technique described previously.^{4,5,14,15} The detailed imaging parameters for HR-SWI were as follows: flow-compensated 3D gradient-echo sequence; TR/TE, 24/34 ms; flip angle, 10°; FOV, 200 × 200 mm; matrix, 332 × 332; section thickness, 3 mm; slab thickness, 135 mm; total acquisition time, 4 minutes 2 seconds.

DSC was performed with a gradient-echo echo-planar sequence during the administration of a standard dose of 0.1 mmol/kg of gadopentetate dimeglumine (Magnevist) per kilogram of body weight at a rate of 4 mL/s with an MR imaging-compatible power injector (Spectris MR injector; MedRad, Indianola, Pa). The bolus of contrast material was followed by a 20-mL bolus of saline, which was administered at the same injection rate. The detailed imaging parameters for DSC were as follows: TR/TE, 1407/40 ms; flip angle, 35°; FOV, 24 cm; matrix, 128 × 128. Total acquisition time for DSC was 1 minute 30 seconds. DSC was performed by using the same section orientations and coverage as those used for conventional MR imaging and HR-SWI. All imaging data were transferred from the scanner to an independent PC for quantitative analysis. Perfusion parametric maps were obtained by using a dedicated software package (nordicICE; NordicImagingLab, Bergen, Norway). After eliminating recirculation of contrast agent with gamma-variate curve fitting, we computed the rCBV by means of a numeric integration of the curve.

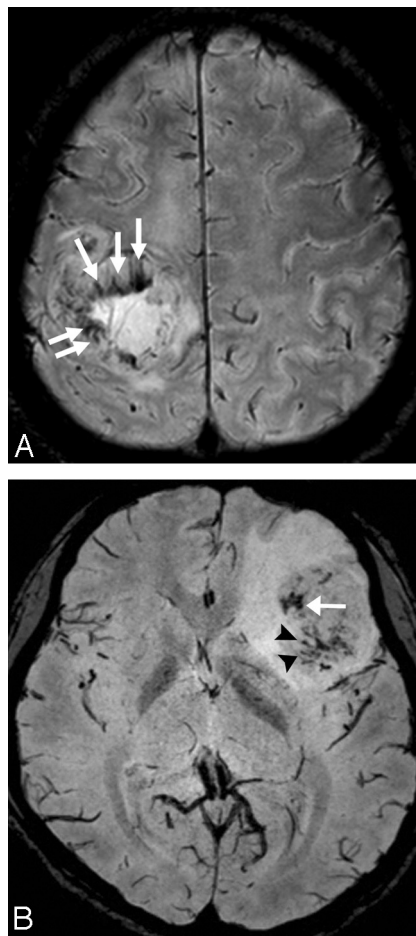


Fig 1. The morphology of ITSS. *A*, Conglomerated fine linear (arrows) ITSSs. *B*, Mixed dots (arrows) and fine linear (arrowheads) ITSSs.

Image Analysis

For qualitative image analysis, conventional MR images and HR-SWIs were assessed by 2 experienced radiologists. Intratumoral calcifications or macrohemorrhages, which could cause susceptibility signals on HR-SWI, were excluded on the basis of low signals in conventional MR imaging, including gradient-echo images, and susceptibility artifacts detected on diffusion-weighted images (DWIs) and DSC images. We detected several microbleeds that were not related to tumor, in the bilateral basal ganglia and thalami, associated with small vessel disease in 2 patients. However, we did not detect any lobar microbleeds, small cavernoma, or incidental calcification on HR-SWI, conventional gradient-echo, DWI, and DSC images.

ITSS was defined as low signal intensity and a fine linear or dotlike structure, with or without conglomeration, seen within the tumor on HR-SWI. We assessed the presence or absence of ITSS in each tumor and compared the incidence of ITSS between high- and low-grade gliomas. We also determined the specific morphology of the ITSS and reached a consensus as to which type was predominantly seen in each high- or low-grade glioma. The morphology of the ITSS was classified into 3 categories: conglomerated dots, conglomerated fine linear structures, and dots mixed with fine linear structures (Fig 1).

For the quantitative or semiquantitative analysis, the degree of ITSS was divided into 4 grades: grade 0, no ITSS; grade one, 1–5 dotlike or fine linear ITSSs; grade two, 6–10 dotlike or fine linear ITSSs; and grade 3, ≥ 11 dotlike or fine linear ITSSs in the continuous area within a tumor. Normalized rCBV maps were calculated on a

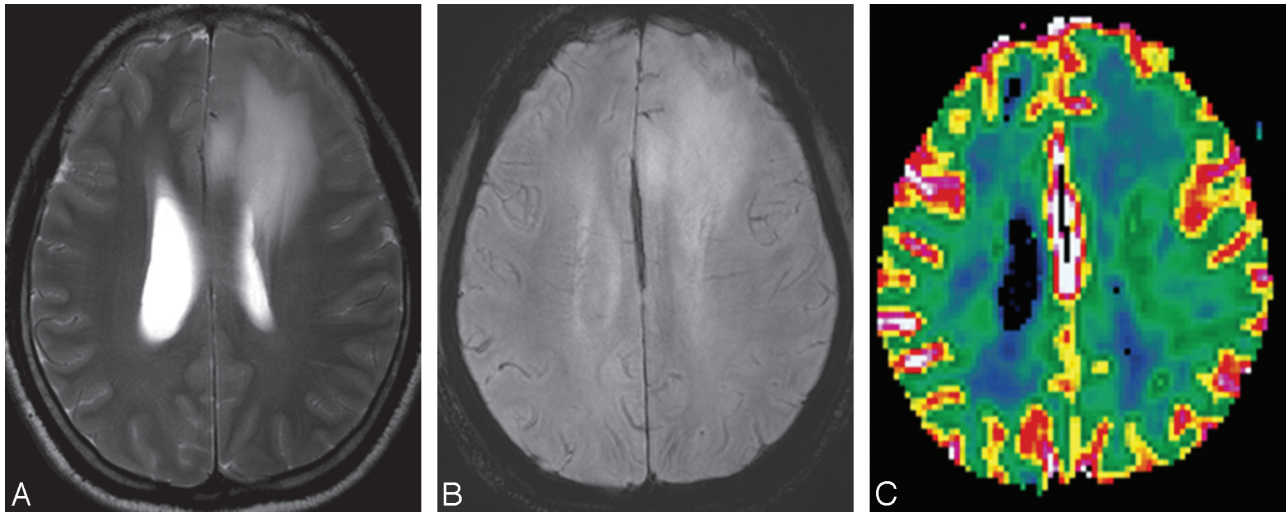


Fig 2. MR images of a 39-year-old woman with left frontal low-grade astrocytoma (WHO grade II). *A*, The axial T2-weighted image shows an ill-defined mass with high signal intensity in the left frontal lobe. *B*, HR-SWI demonstrates no evidence of the ITSS. *C*, Corresponding rCBV map shows relatively low rCBVmax values of 1.31.

pixel-by-pixel basis by dividing pixel rCBV values by the mean rCBV value of the contralateral normal-appearing white matter of the centrum semiovale. The size of the region of interest in the contralateral normal white matter was kept constant (diameter, 3 mm). Coregistration between the HR-SWIs and the normalized rCBV maps was performed on the basis of geometric information stored in the respective datasets. The normalized rCBV maps were displayed as color overlays on the HR-SWIs. Four separate regions of interest were designated in the region of maximum abnormalities within the same tumor segments, including maximum degree of ITSSs as determined visually on the coregistered HR-SWI and rCBV map. The size of the region of interest was kept constant (diameter, 1.5 mm), and the rCBVmax value among the 4 regions of interest was recorded. This maximum value of the region of interest analysis has been reported to provide the highest intraobserver and interobserver reproducibility in MR perfusion measurements.¹⁶

We assessed the level of interobserver variability for the degree of ITSS and rCBVmax measurements and calculated the correlation coefficient between the degree of ITSS and the rCBVmax obtained from DSC. The degree of ITSS and rCBVmax was compared among WHO grades II, III, and IV, and the correlation coefficients between the ITSS degree or rCBVmax and glioma grade were determined. Finally, the sensitivity, specificity, positive predictive value (PPV), and negative predictive value (NPV) of HR-SWI were calculated for the correct identification of high-grade (WHO grades III and IV) and low-grade (WHO grade II) gliomas. The sensitivity and specificity were estimated by using standard statistical formulas and were based on the consensus data from the quantitative measures.

Statistical Analysis

Intraclass correlation coefficient (ICC) was used to determine the levels of interobserver variability in quantitative analysis of ITSS on HR-SWI and MR perfusion parameters. Analysis of variance (ANOVA) and the Kruskal-Wallis test were performed to compare the mean ITSS degree and rCBVmax among 3 groups with different histopathologic grades. Spearman correlation coefficients were used to show the relationships between the degree of ITSS or rCBVmax and histopathologic grades. Receiver operator characteristic (ROC) curve analyses were performed to determine optimum thresholds and diagnostic accuracy of HR-SWI and DSC for ascertaining high-grade tu-

mor. This analysis permitted the calculation of the sensitivity, specificity, PPV, and NPV associated with each parameter of HR-SWI and DSC as a function of the threshold value used to identify high-grade and low-grade gliomas. We analyzed the ROC curve by using MedCalc for Windows (MedCalc Software, Mariakerke, Belgium). The areas under the ROC curves (AUCs) were compared between the HR-SWI and DSC parameters. All *P* values were 2-tailed, with .05 as the criterion for statistical significance.

Results

Of the 41 tumors, 12 were low-grade astrocytomas (WHO grade II), 7 were anaplastic astrocytomas (WHO grade III), and 22 were glioblastoma multiformes (WHO grade IV).

In the qualitative analysis, the ITSSs were seen in 22 (100%) of 22 glioblastoma multiformes (WHO grade IV) and in 3 (43%) of 7 anaplastic astrocytomas (WHO grade III). There was no evidence of ITSS in low-grade astrocytomas (WHO grade II). On HR-SWI, these ITSSs were usually located in the inner portion of the contrast-enhancing rim on contrast-enhanced T1-weighted images. Regarding the morphology of the ITSSs, conglomerated mixed fine linear and dotlike ITSSs were most frequent in glioblastomas, and the fine linear ITSSs were seen in all anaplastic astrocytomas. The fine linear or dotlike ITSSs partly corresponded with the regions of visual rCBVmax on coregistered images of HR-SWI and normalized rCBV maps. However, densely prominent ITSSs did not correspond with the regions of visual rCBVmax.

In the quantitative analysis, interobserver agreement for the degree of ITSS and rCBVmax was excellent for determining the degree of ITSS (ICC = 0.93) and for measuring rCBVmax (ICC = 0.82). The degree of ITSS showed a significant correlation with the value of rCBVmax in the same tumor segments ($r = 0.72$, $P < .0001$; Figs 2–5). The Kruskal-Wallis test showed that the degree of ITSS was significantly different among all 3 grades ($P < .005$). Tables 1 and 2 list the sensitivity, specificity, PPV, and NPV of ITSS degree and rCBVmax for differentiating among the 3 groups with various histopathologic grades. The Spearman correlation coefficient between the degree of ITSS and the glioma grade was 0.88 (95% [CI], 0.79–0.94). In the ROC curve analysis with his-

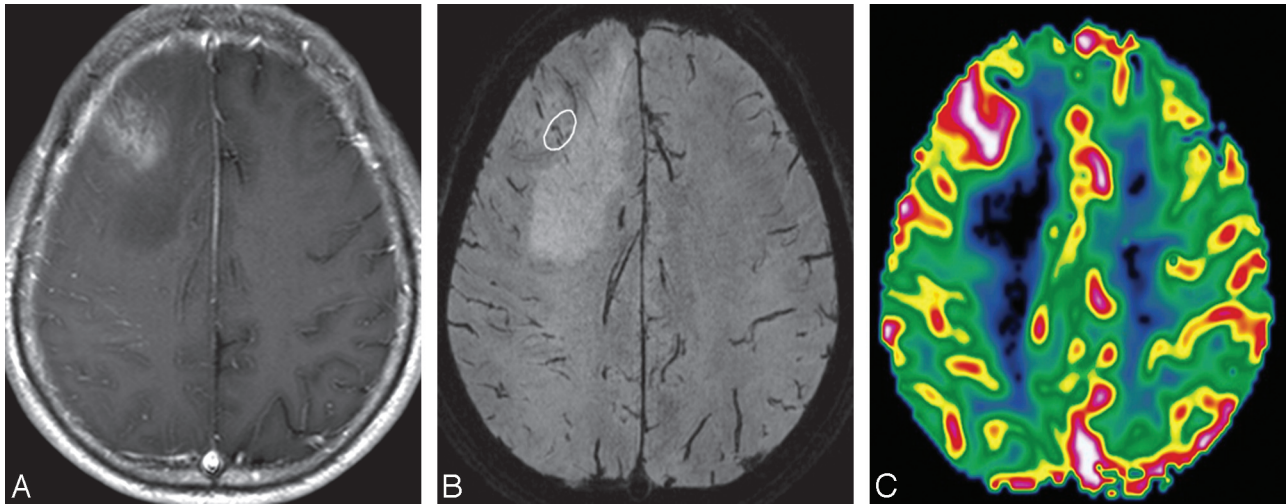


Fig 3. MR images of a 53-year-old man with a right frontal anaplastic astrocytoma. *A*, The contrast-enhanced axial T1-weighted image shows an ill-defined mass with minimal contrast enhancement. *B*, HR-SWI demonstrates a few fine linear and dotlike ITSSs (white circle) in the peripheral area. *C*, Corresponding rCBV map shows a high rCBVmax value of 2.53 in the tumor segment, including maximum degree of ITSS.

topathologic correlation, optimal sensitivity, specificity, PPV, and NPV to determine a high-grade glioma by using the ITSS degree and rCBVmax were 85.2%, 92.9%, 95.8%, and 76.5%, respectively, listed in Table 3, and 92.6%, 85.7%, 92.6%, and 85.7%, respectively, listed in Table 4, (Fig 6).

Discussion

The main finding of this study was that the degree of ITSS showed a significant correlation with the value of rCBVmax in the same tumor segments. On the other hand, the direct correspondence between the areas of ITSS and rCBVmax was variable. The specific morphologic patterns (fine linear and dotlike) of ITSS partly corresponded with the areas of visual rCBVmax. However, the areas of densely prominent ITSSs did not accurately correspond with the areas of visual rCBVmax. HR-SWI demonstrated the highest degree of ITSS in glioblastoma multiformes, suggesting that ITSSs can be a potentially helpful sign for a correct diagnosis of high-grade gliomas. The ITSSs were seen in all glioblastomas, though the degree was somewhat different in each tumor and was never seen in low-grade gliomas (grade II). In anaplastic astrocytomas, the degree of ITSS was variable. We also found that the diagnostic performance of HR-SWI for grading gliomas was comparable with that of DSC. In the ROC curve analysis, the diagnostic accuracy of HR-SWI for determining high-grade glioma was relatively high. The specificity and PPV of the high degree (grade II or more) of ITSS for determining high-grade gliomas were high.

MR perfusion is currently one of the best imaging techniques for the evaluation of glioma grade. The rCBV and K^{trans} have been reported as reliable parameters in glioma grading.⁷⁻⁹ Recently, HR-SWI has been described as a useful tool for noninvasive glioma grading.^{11,12,17} High rCBV values on perfusion imaging in tumors go hand in hand with evidence of blood products detected within the tumor matrix on HR-SWI.¹⁰ On the other hand, probably related to the angiogenesis and increased tumor blood supply, high-grade gliomas contain a relatively large amount of deoxyhemoglobin, which generates susceptibility effects and causes signal-intensity

loss.¹¹ Pinker et al¹² reported that intralesional susceptibility effects were correlated with tumor grade, as determined by PET and histopathology, and that by direct comparison of intralesional susceptibility effects with the histopathology, intratumoral susceptibility effects reflected conglomerates of tumor microvasculature. As described in previous reports,^{10,11} the detection of ITSS in higher grade gliomas not only reflects tumor vascularity but also indicates considerable susceptibility in areas of macro- and micronecrosis in higher grade gliomas. In the present study, the degree of ITSS showed a significant correlation with the value of rCBVmax in the same tumor segments.¹⁰ However, the areas of the highest ITSSs did not accurately correspond with the areas of visual rCBVmax on the coregistered HR-SWI and rCBV maps because ITSS can reflect considerable susceptibility associated with tumor necrosis and microhemorrhage as well as tumor vascularity. The fine linear or dotlike ITSSs partly corresponded with the regions of visual rCBVmax on coregistered images of HR-SWI and rCBV map.

With the advent of 3T MR imaging scanners and parallel imaging techniques, the acquisition time of HR-SWI is not exhaustive, compared with conventional gradient-echo techniques. As shown previously,^{4-6,17} HR-SWI can provide valuable additional information in pathologic brain disorders. Moreover, contrary to a previous report,¹⁷ HR-SWI, as included in our imaging protocol, allowed coverage of the whole brain within the acquisition time mentioned above. At our institution, we could acquire HR-SWI with reasonable spatial resolution within 4 minutes, and our routine brain MR imaging protocol now includes non-contrast-enhanced HR-SWI.

Several previous studies have proposed that HR-SWI should be performed with contrast enhancement, because the contrast agent can shorten T1-relaxation times of blood; therefore, the extra phase shift could improve signal-intensity cancellation at shorter acquisition times and thus result in a shorter scanning time.^{11,12,17} Moreover, Mittal et al¹⁰ proposed that hemorrhages can be easily distinguished from veins if HR-SWI is performed both before and after administration of contrast agent. Blood vessels will change their signal inten-

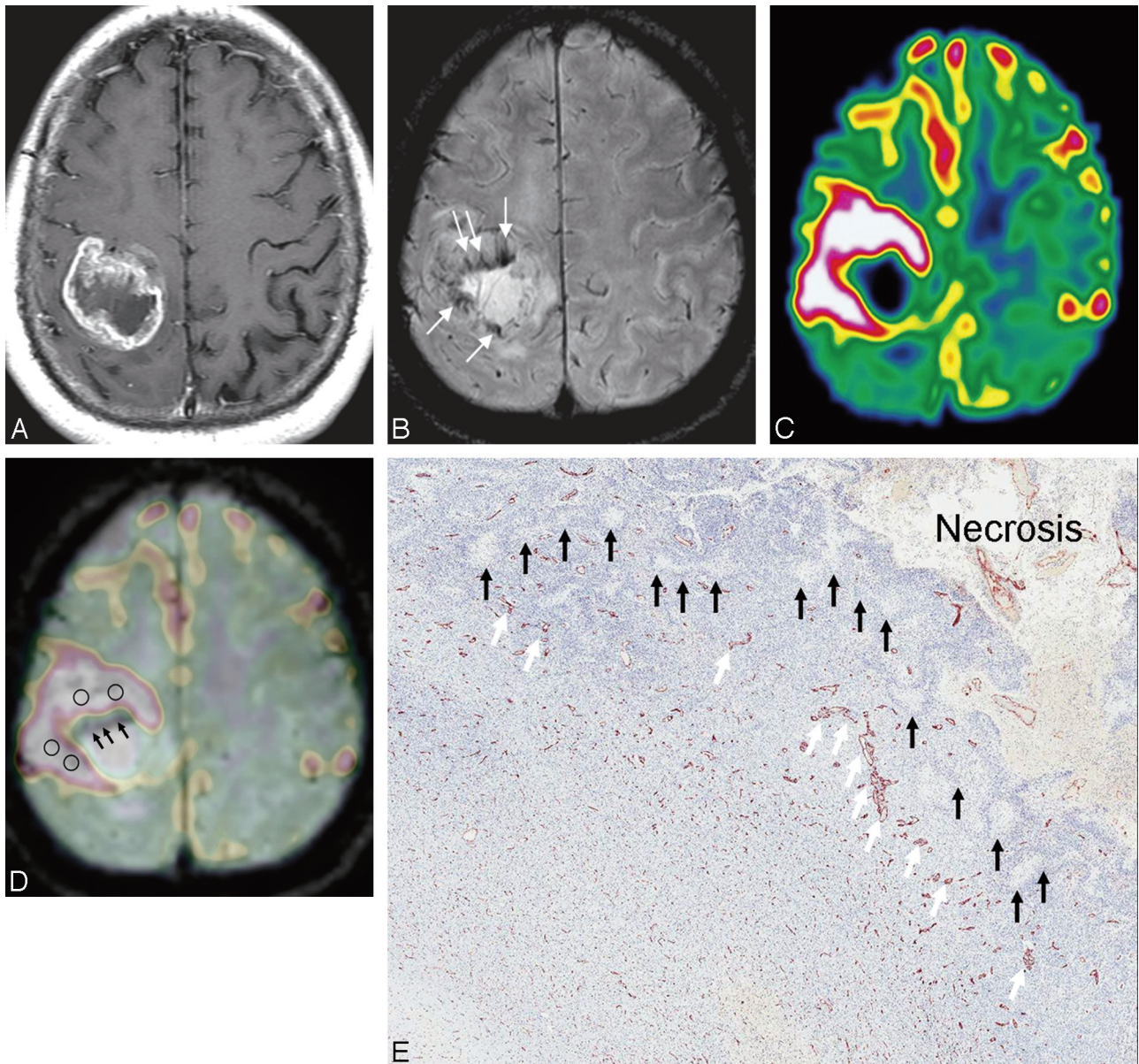


Fig 4. MR images of a 55-year-old man with a glioblastoma multiforme. *A*, The contrast-enhanced axial T1-weighted image shows a mass with irregular peripheral rim enhancement in the right parietal lobe. *B*, HR-SWI reveals conglomerated fine linear ITSSs just in the inner portion of the enhancing rim on the contrast-enhanced T1-weighted image. *C*, Corresponding rCBV map shows high rCBVmax values (4.71) in the tumor segment, including a maximum degree of ITSS. *D*, Coregistered image of HR-SWI and rCBV shows that the area of attenuated prominent ITSSs (arrows) does not correspond with the area of visual rCBVmax, and the area of fine linear ITSSs partly corresponds with the area of visual rCBVmax. *E*, Corresponding histopathologic specimen (CD34 vessel staining, original magnification $\times 10$) demonstrates pseudopalisading necrosis (black arrows) and tumor vessels (white arrows).

sity due to the contrast agent, but signal intensity from hemorrhage will not change.¹⁰ However, routine MR imaging protocols for brain tumors usually include contrast-enhancement studies such as contrast-enhanced T1-weighted imaging and perfusion MR imaging. Therefore, the combination of HR-SWI and contrast enhancement does not provide an added value in diagnostic accuracy or acquisition time for glioma grading. In the present study, we performed HR-SWI without contrast administration. If the diagnostic accuracy of noncontrast-enhanced HR-SWI for glioma grading was comparable with that of perfusion MR, currently the best imaging technique for glioma grading, we would expect that a non-contrast-enhanced MR imaging protocol could be performed in routine brain tumor imaging. In the present study, the diagnostic accuracy, including sensitivity and specificity, of non-

contrast-enhanced HR-SWI for glioma grading was comparable with that of DSC.

Our study has several limitations. First, the T2* first-pass technique is fairly sensitive to minor susceptibility in the tissue being examined; therefore, the rCBV measurements would be unreliable in areas of considerable ITSS. In the present study, the regions of attenuated prominent ITSS that could reflect considerable susceptibility associated with tumor necrosis and microhemorrhage did not accurately correspond with the region of rCBVmax on the coregistered HR-SWI and rCBV maps. Second, of the 41 patients, 12 underwent stereotactic biopsy, which might be prone to the sampling error of not including the most representative part of the tumor. However, we decided the biopsy site on the basis of information from both contrast enhancement and foci of rCBVmax values. It has

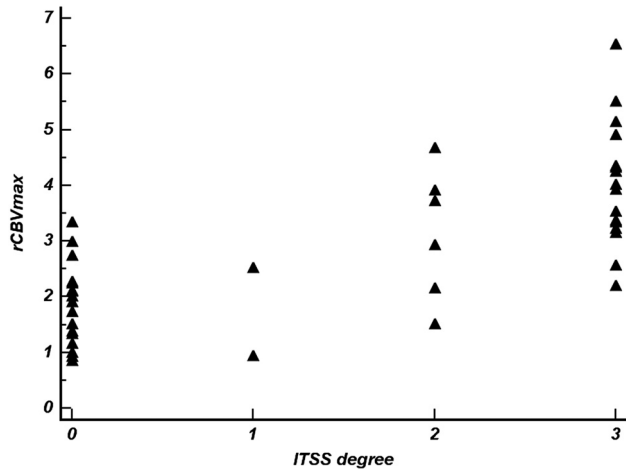


Fig 5. Scatterplot shows the correlation between the degree of ITSS and rCBVmax within the same tumor segment ($r = 0.72$; 95% CI, 0.53–0.84).

Table 1: Sensitivity, specificity, PPV, and NPV of ITSS degree for differentiating WHO grade II, III, and IV gliomas

Glioma Grade	Sensitivity	Specificity	PPV	NPV
II vs III	50.0%	92.9%	80.0%	76.5%
II vs IV	100.0%	100.0%	100.0%	100.0%
III vs IV	78.9%	87.5%	93.8%	63.6%

Note:—PPV indicates positive predictive value; NPV, negative predictive values; ITSS, intratumoral susceptibility signal intensity.

Table 2: Sensitivity, specificity, PPV, and NPV of rCBVmax for differentiating WHO grade II, III, and IV gliomas

Glioma Grade	Sensitivity	Specificity	PPV	NPV
II vs III	87.5%	71.4%	63.6%	90.9%
II vs IV	100.0%	85.7%	90.5%	100.0%
III vs IV	89.5%	75.0%	89.5%	75.0%

Note:—rCBVmax indicates maximum relative cerebral blood volume.

Table 3: Sensitivity, specificity, PPV, and NPV of ITSS degree for determining high-grade gliomas (WHO grades III and IV) according to threshold values

Criterion	Sensitivity	Specificity	PPV	NPV
$\geq 1^*$	85.2%	92.9%	95.8%	76.5%
≥ 2	81.5%	100.0%	100.0%	73.7%

* Value indicates optimum threshold value.

Table 4: Sensitivity, specificity, PPV, and NPV of rCBVmax for determining high-grade gliomas (WHO grades III and IV) according to threshold values

Criterion	Sensitivity	Specificity	PPV	NPV
< 1.92	96.3%	71.4%	86.7%	90.9%
< 2.02	92.6%	71.4%	86.2%	83.3%
$< 2.12^*$	92.6%	85.7%	92.6%	85.7%

* Value indicates optimum threshold value.

been reported that this approach may offer a more accurate way of choosing a biopsy site.¹⁸

Third, we performed a direct correlation between HR-SWI–derived ITSS and histopathologic findings in only 3 of our patients. However, the direct histopathologic correlation has previously been reported⁸; therefore, we focused on the comparison of HR-SWI with DSC. Fourth, we did not have

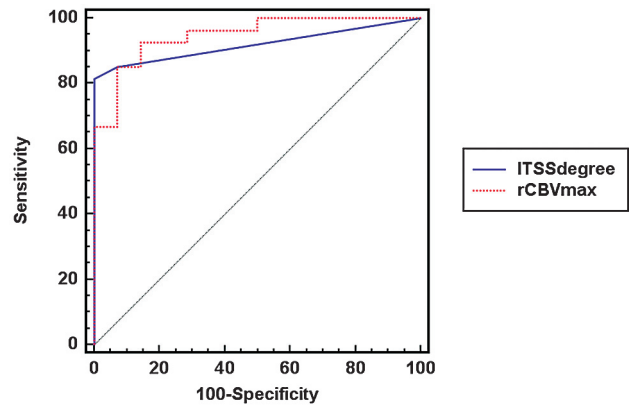


Fig 6. The comparison of ROC curve analysis between the degree of ITSS and rCBVmax for correctly identifying a high-grade glioma (WHO grades III and IV). The AUC for the degree of ITSS is 0.919 (95% CI, 0.790–0.980) and that for the rCBVmax is 0.947 (95% CI, 0.828–0.991). The P value for the difference between the 2 AUCs is .54.

any guidelines or references for the morphologic classification of ITSS and the quantification of the degree of ITSS; thus, our method could be subjective. However, the interobserver agreement for our measurement of the ITSS degree was excellent. Finally, an uneven distribution of tumor grades was used for our analysis. The current study included a relatively small number of anaplastic astrocytomas (WHO grade III). For practical purposes, we grouped patients with anaplastic astrocytomas and glioblastoma multiformes together in our major analysis. Further studies with larger populations are necessary to determine the usefulness of HR-SWI in differentiating these 2 tumor groups.

Conclusions

The degree of ITSS showed a significant correlation with the value of rCBVmax in the same tumor segments. However, the direct correspondence between the areas of ITSS and rCBVmax was variable, according to the morphology and degree of ITSSs. The diagnostic performance of HR-SWI for glioma grading is comparable with that of DSC. Therefore, the ITSS can be a potentially helpful sign suggesting a correct diagnosis of high-grade glioma. Our results show the possibility of a noncontrast brain tumor imaging protocol in patients who have contraindications for contrast agents or who cannot tolerate the bolus injection.

References

- Reichenbach JR, Jonetz-Mentzel L, Fitzek C, et al. High-resolution blood oxygen-level dependent MR venography (HRBV): a new technique. *Neuroradiology* 2001;43:364–69
- Reichenbach JR, Essig M, Haacke EM, et al. High-resolution venography of the brain using magnetic resonance imaging. *MAGMA* 1998;6:62–69
- Reichenbach JR, Haacke EM. High-resolution BOLD venographic imaging: a window into brain function. *NMR Biomed* 2001;14:453–67
- Sehgal V, Delproposto Z, Haacke EM, et al. Clinical applications of neuroimaging with susceptibility-weighted imaging. *J Magn Reson Imaging* 2005;22:439–50
- Lee BC, Vo KD, Kido DK, et al. MR high-resolution blood oxygenation level-dependent venography of occult (low-flow) vascular lesions. *AJNR Am J Neuroradiol* 1999;20:1239–42
- de Souza JM, Domingues RC, Cruz LC Jr, et al. Susceptibility-weighted imaging for the evaluation of patients with familial cerebral cavernous malformations: a comparison with T2-weighted fast spin-echo and gradient-echo sequences. *AJNR Am J Neuroradiol* 2008;29:154–58
- Lev MH, Ozsunar Y, Henson JW, et al. Glial tumor grading and outcome pre-

- diction using dynamic spin-echo MR susceptibility mapping compared with conventional contrast-enhanced MR: confounding effect of elevated rCBV of oligodendrogliomas. *AJNR Am J Neuroradiol* 2004;25:214–21
8. Law M, Yang S, Wang H, et al. Glioma grading: sensitivity, specificity, and predictive values of perfusion MR imaging and proton MR spectroscopic imaging compared with conventional MR imaging. *AJNR Am J Neuroradiol* 2003;24:1989–98
 9. Law M, Yang S, Babb JS, et al. Comparison of cerebral blood volume and vascular permeability from dynamic susceptibility contrast-enhanced perfusion MR imaging with glioma grade. *AJNR Am J Neuroradiol* 2004;25:746–55
 10. Mittal S, Wu Z, Neelavalli J, et al. Susceptibility-weighted imaging: technical aspects and clinical applications, part 2. *AJNR Am J Neuroradiol* 2009;30:232–52. Epub 2009 Jan 8
 11. Pinker K, Noebauer-Huhmann IM, Stavrou I, et al. High-resolution contrast-enhanced, susceptibility-weighted MR imaging at 3T in patients with brain tumors: correlation with positron-emission tomography and histopathologic findings. *AJNR Am J Neuroradiol* 2007;28:1280–86
 12. Barth M, Nobauer-Huhmann IM, Reichenbach JR, et al. High-resolution three-dimensional contrast-enhanced blood oxygenation level-dependent magnetic resonance venography of brain tumors at 3 Tesla: first clinical experience and comparison with 1.5 Tesla. *Invest Radiol* 2003;38:409–14
 13. Daumas-Duport C, Beuvon F, Varlet P, et al. Gliomas: WHO and Sainte-Anne Hospital classifications. *Ann Pathol* 2000;20:413–28
 14. Haacke EM, Xu Y, Cheng YC, et al. Susceptibility-weighted imaging (SWI). *Magn Reson Med* 2004;52:612–18
 15. Rauscher A, Sedlacik J, Barth M, et al. Magnetic susceptibility-weighted MR phase imaging of the human brain. *AJNR Am J Neuroradiol* 2005;26:736–42
 16. Wetzel SG, Cha S, Johnson G, et al. Relative cerebral blood volume measurements in intracranial mass lesions: interobserver and intraobserver reproducibility study. *Radiology* 2002;224:797–803
 17. Pinker K, Noebauer-Huhmann IM, Stavrou I, et al. High-field, high-resolution, susceptibility-weighted magnetic resonance imaging: improved image quality by addition of contrast agent and higher field strength in patients with brain tumors. *Neuroradiology* 2008;50:9–16
 18. Covarrubias DJ, Rosen BR, Lev MH. Dynamic magnetic resonance perfusion imaging of brain tumors. *Oncologist* 2004;9:528–37